

# Absolute Optical Frequency Measurements with a Fractional Frequency Uncertainty at $1 \times 10^{-15}$

J.E. Stalnaker, S.A. Diddams, K. Kim, L. Hollberg,  
E.A. Donley, T.P. Heavner, S.R. Jefferts, F. Levi,  
T.E. Parker, J.C. Bergquist, W.M. Itano, M.J. Jensen,  
L. Lorini, and W.H. Oskay  
Time and Frequency Division MS 847  
National Institute of Standards and Technology  
Boulder CO 80305

T.M. Fortier  
P-23 Physics Division MS H803  
Los Alamos National Laboratory  
Los Alamos NM 87545

**Abstract**— We report the technical details specific to our recent measurements of the optical frequency of the mercury single-ion frequency standard in terms of the SI second as realized by the NIST-F1 cesium fountain clock. In these measurements the total fractional uncertainty is  $\approx 10^{-15}$ , limited by the statistical measurement uncertainty. In this paper we will address the techniques employed for the optical-to-microwave comparison itself, which had an estimated fractional uncertainty of  $\sim 3 \times 10^{-16}$ , limited by the stability of the electronics used for the comparison.

## I. INTRODUCTION

The development of femtosecond laser frequency combs (FLFCs) has led to a dramatic simplification of the absolute measurement of optical frequencies. By providing the necessary division of optical frequencies at hundreds of terahertz to rf and microwave standards at the gigahertz frequency range, frequency combs have made measurements of optical frequencies routine (for reviews, see [1], [2]). However, only a few absolute frequency measurements have been made at levels approaching the uncertainty of the best cesium (Cs) fountain frequency standards [3]–[8]. Achieving accuracies in measurements of optical frequency standards that approach those of the Cs standards is an essential step towards the next generation of optical frequency standards.

This paper discusses an optical-to-microwave comparison between the mercury ion ( $\text{Hg}^+$ ) optical frequency standard and the microwave Cs fountain frequency standard, NIST-F1. The uncertainty in the measurement of the absolute frequency of the optical  $\text{Hg}^+$  transition has reached a fractional level of  $\approx 1 \times 10^{-15}$  [3], [4]. This uncertainty is within a factor of  $\approx 2.3$  of the current uncertainty in the NIST-F1 frequency standard [9], [10]. Here we focus on the techniques used to relate the two frequencies, discuss limitations on the optical-to-microwave conversion process, and compare the uncertainties arising in the measurement process to those of the frequency standards.

## II. EXPERIMENT

An overview of the frequency comparison method is shown in Fig. 1. The frequency of the two standards are each measured with respect to the same hydrogen maser. The frequency

of the Cs standard provides a calibration of the maser and the FLFC provides the conversion of the  $\text{Hg}^+$  optical frequency to an rf frequency that can be compared to the maser.

The frequency of the Cs standard is measured with respect to the output of a 9.2 GHz synthesizer which, in turn, is referenced to a stable quartz crystal. The frequency of the quartz crystal is steered to the frequency of a hydrogen maser. The output of a direct digital frequency synthesizer (DDS) is combined with the output of a direct digital frequency synthesizer (DDS) to generate the frequency to match the Cs resonance. The amount by which the DDS shifts the frequency from its nominal value is recorded and provides a calibration of the hydrogen maser frequency. These deviations from the nominal value are added to a frequency near 10 MHz with a second DDS and sent to the FLFC laboratory, where they are measured with a frequency counter.

By use of the FLFC, the frequency of the  $\text{Hg}^+$  standard is simultaneously measured with respect to a 1 GHz synthesizer that is referenced to the same quartz crystal and calibrated maser. The light used in the  $\text{Hg}^+$  experiment is interfered with the FLFC to form a heterodyne beat signal between the  $\text{Hg}^+$  light and a single mode of the FLFC. This beat signal is used to phase lock a single mode of the FLFC. With the carrier-envelope offset frequency also stabilized, the repetition rate of the FLFC is directly related to the  $\text{Hg}^+$  frequency. This repetition rate is compared to the 1 GHz synthesizer. The difference in the frequency of the repetition rate and the 1 GHz synthesizer is recorded with a frequency counter. With the carrier-envelope offset frequency, the heterodyne beat frequency of the  $\text{Hg}^+$  light and the FLFC, and the repetition rate known, the frequency of the  $\text{Hg}^+$  frequency with respect to the hydrogen maser can be computed.

In addition, the stabilized carrier-envelope offset frequency and the frequency of the phase lock between the  $\text{Hg}^+$  light and FLFC are counted to monitor possible phase slips in the locks.

The ratio of the frequency of the  $\text{Hg}^+$  standard with respect to Cs is determined by taking the ratio of the two frequencies measured with respect to the hydrogen maser.

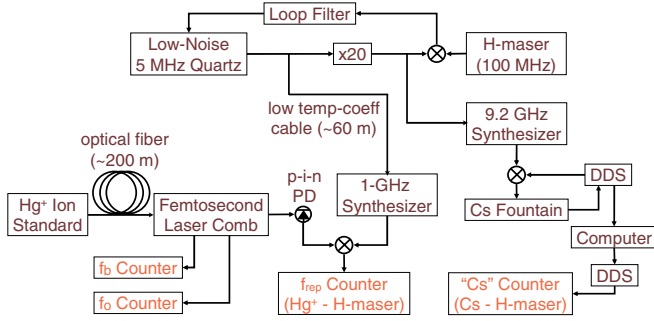


Fig. 1. Block diagram showing the relations of the frequencies used in the  $\text{Hg}^+$  /Cs comparison. The frequency of the DDS is added to the 9.2-GHz synthesizer to generate the frequency of the Cs resonance. This small correction is added to a second DDS and sent to the FLFC laboratory to be counted. With the comb stabilized to the  $\text{Hg}^+$  light and the carrier-envelope offset frequency stabilized, the repetition rate of the comb can be related to the  $\text{Hg}^+$  frequency.

### A. Cs Frequency Standard

The Cs frequency standard used for these measurements was the Cs fountain clock NIST-F1. Detailed descriptions of NIST-F1 as well as its accuracy evaluations are given in Refs. [9]–[11]. Here we discuss only those features that are specific for this experiment.

The Cs standard is operated at varying densities in order to balance the statistics with the systematic effects arising from spin-exchange collisions [11]. For this work the Cs standard was operated at a density approximately seven times higher than that used for the majority of the data collected during its accuracy evaluations. At this density the frequency standard has a fractional frequency instability of  $2 \times 10^{-13} \tau^{-1/2}$ , where  $\tau$  is the averaging time in seconds, and an uncertainty of  $0.33 \times 10^{-15}$  due to spin-exchange collisions only [9], [10]. Under the conditions used for this measurement, the total uncertainty in the Cs standard was  $0.41 \times 10^{-15}$ .

### B. $\text{Hg}^+$ Frequency Standard

The  $^{199}\text{Hg}^+$  frequency standard is based on the  $5d^{10}6s^2S_{1/2} \rightarrow 5d^96s^2^2D_{5/2}$  transition at  $1.065 \times 10^{15}$  Hz [?], [12]. The radiation for the clock transition is generated by frequency quadrupling light at 266 THz from a fiber laser. The doubled light at 532 THz is pre-stabilized to a low drift, high-finesse optical cavity and then steered to resonance with the  $\text{Hg}^+$ .

Some of the stabilized light is sent through  $\approx 200$  m of single mode optical fiber to the femtosecond frequency comb. The frequency noise introduced by the fiber is suppressed by standard fiber-noise canceling techniques [13].

### C. Optical-to-Microwave Conversion

The division of the optical frequency from the  $\text{Hg}^+$  standard to a rf frequency that can be related to the hydrogen maser, and therefore to the Cs standard, is accomplished with the FLFC. The FLFC generates a comb of  $\approx 10^5$  frequencies, each of which is exactly related to two rf frequencies by

$$\nu_n = f_{ceo} + n f_{rep}, \quad (1)$$

where  $f_{ceo}$  is the carrier-envelope offset frequency and  $f_{rep}$  is the repetition rate. The carrier-envelope offset frequency sets the absolute position of the comb and is determined from the laser cavity dispersion [14]. The repetition rate  $f_{rep}$ , defines the spacing of the frequency components of the comb and is set by the cavity length. The stabilization of any two frequency components of the comb results in the stabilization of the entire comb.

For the  $\text{Hg}^+$  comparison to the Cs standard, the carrier-envelope offset frequency and a single-frequency mode of the comb were stabilized (Fig. 2).

The comb used in the most recent measurements of the  $\text{Hg}^+$  frequency is described in detail in [15]. The laser is a mode-locked laser based on Ti:Sapphire with a repetition rate of  $\approx 1$  GHz. The output of the laser spans an optical octave, allowing for the stabilization of the carrier-envelope offset frequency with a  $f$ -to- $2f$  self-referencing technique [16]. Part of the optical spectrum at  $\approx 1100$  nm was frequency doubled and compared to the light directly produced by the laser at  $\approx 550$  nm. The doubled light and the direct light were interfered on a photomultiplier tube, resulting in a heterodyne beat signal, the frequency of which equals the carrier-envelope offset frequency. The beat frequency can be coarsely adjusted by tilting a 1 mm piece of fused silica inside the laser cavity to change the cavity dispersion, and is servo-controlled by changing the power of the laser pumping the FLFC by use of an acousto-optic modulator (AOM).

The comb was generally operated with the carrier-envelope offset frequency phase locked at  $\approx 50$  MHz. The signal-to-noise ratio of the beat signal was  $\approx 30$  dB in a 300 kHz resolution bandwidth. The detected beat note was filtered by a tunable bandpass filter, amplified, and then mixed up to a higher frequency,  $\approx 1.2$  GHz, and filtered through an rf cavity bandpass filter. The frequency of this signal was then divided by eight and sent to a digital phase detector, with a second synthesizer, operating at  $\approx 150$  MHz, serving as the local oscillator. The error signal from the digital phase detector was conditioned with a loop filter and then sent to drive the amplitude of an rf signal controlling the pump power via an AOM. The carrier-envelope offset frequency was directly counted with a frequency counter to monitor for possible phase slips in the lock.

In order to achieve sufficient power and a clean spatial mode for the comparison with the  $\text{Hg}^+$  light at 563 nm, part of the laser spectrum was broadened in nonlinear microstructure fiber [17]. The output of the microstructure fiber was combined with the  $\text{Hg}^+$  light and interfered on a high-speed ( $\approx 300$  MHz) photodiode. The  $\text{Hg}^+$  light interferes with the different frequency components of the comb to produce a series of beat frequencies. The lowest heterodyne beat frequency was phase locked to a fixed frequency set by a synthesizer. The beat frequency was typically between 35 and 200 MHz, and the signal-to-noise ratio was  $\approx 30$  dB in a 300 kHz resolution bandwidth. The beat note was filtered, amplified, and sent to a digital phase detector that included a 16-times divider. The error signal from the digital phase detector was sent to a loop



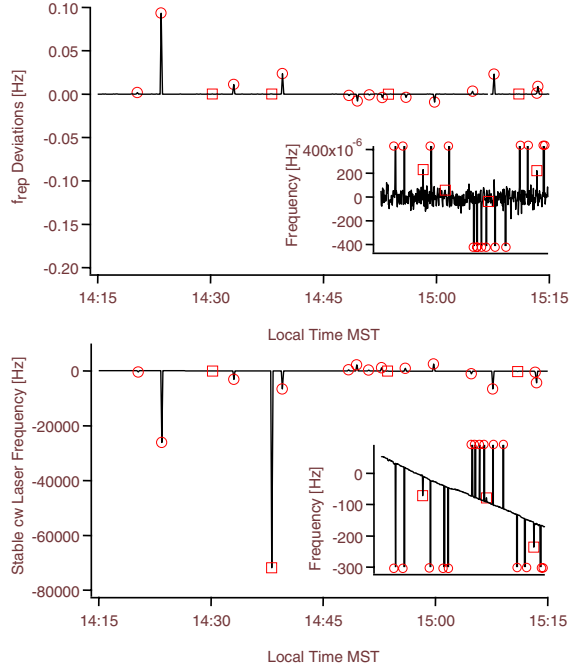


Fig. 3. Relative frequencies of  $f_{rep}$  and the stable cw laser for a representative hour of the data. Upper plot shows the relative frequency of  $f_{rep}$  offset from 1 GHz. Lower plot shows the relative frequency of the stable cw laser offset from 281 THz. The circles indicate data that were considered outliers based on excursions in the repetition rate. Squares indicate data that were considered outliers based only on deviations in the stable cw laser. Insets show the same data with decreased frequency range.

the FLFC generally remained phase locked to the  $\text{Hg}^+$  laser. The frequency deviations were related to a flaw in the laser system and were not due to any instability in the  $\text{Hg}^+$  clock. In addition, there were occasional phase slips of the various locks throughout the experiment. Given these anomalous frequency excursions, the data processing is necessarily focused on determining which of the frequency excursions are intrinsic to the two frequency standards or measurement process and which are a result of imperfections in the experiment.

The frequency excursions present in the  $\text{Hg}^+$  light led to excursions in the frequency of the repetition rate measured relative to the hydrogen maser that was used to determine the frequency of the  $\text{Hg}^+$  transition. These excursions were also present in the measurement of the frequency of the stable cw laser at 1068 nm. The relative fractional frequency instability between the  $\text{Hg}^+$  light and the stable cw laser was  $\approx 2 \times 10^{-15}$  in ten seconds, while the relative fractional frequency instability of the  $\text{Hg}^+$  light and the hydrogen maser was  $\approx 5 \times 10^{-14}$  in ten seconds. Consequently, the frequency of the stable cw laser provides a significantly more sensitive monitor for anomalous frequency excursions. Figure 3 shows one hour of unprocessed data for the repetition rate and the stable cw laser, along with the data points that were considered anomalous excursions based on deviations in the repetition rate and the stable cw laser frequency.

Data that had an anomalous frequency excursion in any of

the recorded frequencies were discarded. Cycle slips that occurred in either the heterodyne beat frequency of the  $\text{Hg}^+$  light with the comb or in the phase lock of the carrier-envelope offset frequency were clearly identified with the counted record of the two frequencies. For the glitches due to other sources, deviations in both the recorded repetition rate and the stable cw laser were used to determine which frequency points were discarded. The criteria for the maximum allowable deviation were varied to determine the sensitivity of the final result on the data analysis. For the final analysis data deviating by more than six times the standard deviation were discarded. An additional complication was introduced when using the frequency of the stable cw laser as a monitor. While the cw laser was more sensitive to frequency excursions, the long-term drift of the cavity prevented use of the deviation from the mean as the criterion for identifying the outlying data. The data for the stable cw-laser frequency were analyzed by looking for local deviations, either by looking at the difference between the recorded frequency and the average frequency of nearby points, or by simply looking for deviations in adjacent frequency points. In addition to excluding data that exhibited large frequency excursions, the data immediately preceding and following the anomalous point were discarded in order to ensure the frequency excursion was completely removed.

The phase-locked  $f_{ceo}$  and  $f_b$  frequencies are additive in the determination of the  $\text{Hg}^+$  frequency. Thus, the fractional deviations in these frequencies are equal to the measured excursion divided by the frequency of the  $\text{Hg}^+$  light measured, 532 THz, while the fractional deviations in  $f_{rep}$  and the Cs steers are normalized by 1 GHz and 9.2 GHz, respectively. The filtered time record of the fractional deviations in the counted signals taken with the 9.472 s counter gate time is shown in Fig. 4.

Varying the cutoff criteria between 6-15 sigma and keeping or discarding adjacent points changed the amount of data discarded from 11 – 38%. However, the final results were statistically consistent. Overall, the variation of the final result with the separate analyses employing different filtering criteria was  $\approx 0.04 \times 10^{-15}$ . We adopt this as an estimate of the uncertainty introduced in the analysis process.

#### IV. UNCERTAINTY ANALYSIS AND FINAL RESULTS

In this section we discuss the frequency corrections and uncertainties affecting the comparison of the two standards. We focus on the uncertainties associated with the optical-to-microwave conversion, mentioning the uncertainties from the Cs and  $\text{Hg}^+$  standards only for reference. Detailed discussions of the uncertainties in the Cs and  $\text{Hg}^+$  standards can be found in Refs. [9]–[11] and [4], respectively.

##### A. Cs Biases and Standard Uncertainties

The Cs frequency measured by the fountain relative to the hydrogen maser must be corrected in order to arrive at the unbiased Cs frequency. The largest bias of the NIST-F1 fountain is from the second-order Zeeman shift caused by the small magnetic field applied to the atoms in the fountain. To

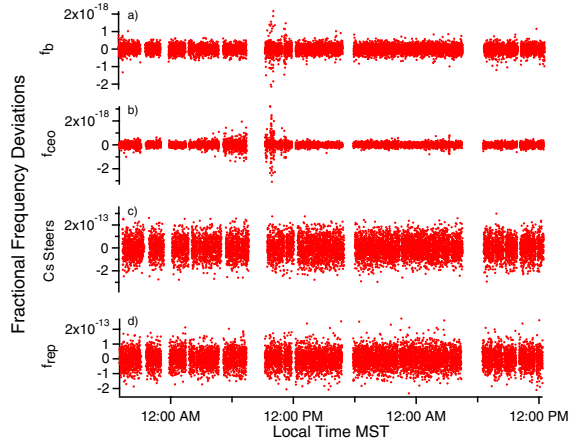


Fig. 4. Time record of the counted fractional frequency deviations for a) phase-locked optical beat between  $\text{Hg}^+$  light and FLFC, b) phase-locked carrier-envelope offset frequency c) Cs frequency relative to hydrogen maser, d) repetition rate of FLFC. The gate time of the counters for this data was 9.472 s and there are 10289 points.

correct for this effect, the fractional frequency is shifted by  $-36.2(1) \times 10^{-15}$ .

The second largest correction comes from the blackbody radiation. The NIST-F1 apparatus is at room temperature and the ambient blackbody radiation leads to ac-Stark shifts of the Cs hyperfine transition energy. These effects have been modeled and are corrected with a fractional shift in the frequency of  $21.2(3) \times 10^{-15}$ .

Finally, the frequency of the Cs standard is shifted due to the spin-exchange collisions of the Cs atoms. For the densities used in the experiment the correction of the fractional frequency shift due to spin-exchange effects was  $2 \times 10^{-15}$  with a fractional uncertainty of  $0.36 \times 10^{-15}$ .

The total fractional correction applied to the frequency of the Cs standard relative to the hydrogen maser was  $-13.0 \times 10^{-15}$ . The total fractional frequency uncertainty in the Cs frequency standard is estimated to be  $0.41 \times 10^{-15}$  [9], [10].

### B. $\text{Hg}^+$ Biases and Standard Uncertainties

The statistical uncertainties of the  $\text{Hg}^+$  standard have been discussed in detail in [4]. The systematic fractional frequency uncertainties are estimated to be  $< 0.7 \times 10^{-15}$ . The only known bias introduced in the  $\text{Hg}^+$  frequency is due to the second-order Zeeman effect and leads to a fractional frequency shift of  $1.1 \times 10^{-15}$ .

### C. Gravitational Shift

The  $\text{Hg}^+$  clock is located one floor below the Cs standard and the FLFC. This difference in altitude gives a relative gravitational shift in the absolute frequency of the  $\text{Hg}^+$  standard relative to the Cs standard. Based on the measured height difference, we apply a fractional correction of  $+0.524(11) \times 10^{-15}$  to the measured frequency of the  $\text{Hg}^+$  standard.

### D. FLFC Optical-to-Microwave Conversion Uncertainties

1) *Optical Uncertainties:* The stability and accuracy of optical synthesis process achieved with similar optical frequency combs has been tested to the  $10^{-19}$  level by comparing two independent frequency combs phase locked to a common cw source [20]. There have been additional tests of the accuracy of the optical synthesis process that included sum and difference frequency generation using nonlinear crystals [21].

We tested the optical synthesis of the frequency comb used in this experiment by comparing the frequency of light from second-harmonic generation in a nonlinear crystal with the fundamental light. Light at 1064 nm from a cw Nd:Yag laser was frequency-doubled with a periodically poled lithium niobate crystal. The frequency comb was stabilized in a manner similar to that used for the  $\text{Hg}^+$ /Cs comparison, with the  $\text{Hg}^+$  light replaced by the frequency-doubled light at 532 nm. With the comb stabilized, the frequency of the 1064 nm light was measured in the same way as was done for the stable cw light used in the  $\text{Hg}^+$  measurement.

Since the two optical frequencies are harmonically related, frequency noise in the doubled light should track the frequency noise in the laser, resulting in rejection of most of the common-mode noise. The remaining fractional instability places an upper limit on instabilities in the optical synthesis process due to frequency noise in the optical interference process, microstructure fiber, and phase locks of the laser. In addition, the accuracy of the optical synthesis process is tested by reproducing the exact ratio of the optical frequencies.

We observed a fractional instability in the fundamental light relative to the doubled light of  $2 \times 10^{-17}$  in one second that averaged down slightly faster than  $\tau^{-1/2}$  (Fig. 5). The ratio of the two frequency components was correct within a counter-limited uncertainty of  $6 \times 10^{-19}$ .

Counting the frequencies of the carrier-envelope offset frequency and the heterodyne beat signal between the  $\text{Hg}^+$  light and the comb provide a limit on uncertainties introduced in the servo process. Both of these locks have an in-loop fractional frequency instability of less than  $3 \times 10^{-19}$  in ten seconds.

2) *Photodetection Uncertainties:* While the optical stability of the comb is far below the statistical uncertainties of both of the frequency standards, the photodetection of the repetition rate introduces additional phase noise. This additional noise is a result of many different processes inherent in the conversion of the short optical pulse ( $\sim 100$  fs) to a much slower electronic signal ( $\sim 1$  ns), such as the conversion of amplitude noise to phase noise, saturation effects within the photodiode and laser-beam pointing noise [22].

The instability introduced due to this detection has been measured with similar detectors and combs and is estimated to be  $\approx 3 \times 10^{-17}$  [23] (Fig. 5).

3) *Electronic Uncertainties:* The stability of the synthesizer used to relate the Cs standard to the hydrogen maser was tested by comparing its frequency to a comparable synthesizer. The fractional stability was found to be  $\approx 10^{-14}$  in one second (Fig. 5) [24].

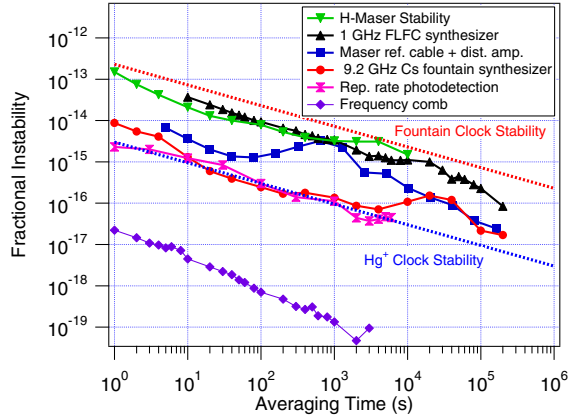


Fig. 5. Frequency instabilities of the main components of the  $\text{Hg}^+$  comparison. See text for a detailed discussion on how the different stabilities were determined

An upper limit on the stability of the 1-GHz synthesizer that was used to compare the FLFC repetition rate to the maser frequency (Fig. 1) was determined by mixing the output of the synthesizer with a second synthesizer referenced to the same maser. The relative fractional frequency instability of the two synthesizers was  $3 \times 10^{-14}$  in ten seconds and averaged down as  $\tau^{-1/2}$  (Fig. 5). The two synthesizers had uncertainties at a level of less than  $3 \times 10^{-16}$ .

In order to limit temperature drifts affecting the output frequency of the synthesizer, the synthesizer was enclosed in an insulated box through which cold water was circulated. The temperature inside the box was monitored throughout the experiment. The temperature dependence of the synthesizer was also tested. A rapid change in the temperature of the synthesizer was introduced and the frequency of the synthesizer relative to a second synthesizer was recorded. The synthesizer was measured to have a fractional frequency change of  $6.0(1.4) \times 10^{-15} (K/hr)^{-1}$ . This temperature coefficient was used, along with the recorded temperature of the synthesizer, to correct the measured repetition rate for drifts in the synthesizer frequency. The correction resulted in a fractional shift of the  $\text{Hg}^+$  frequency of  $0.08(2) \times 10^{-15}$ .

The distribution amplifier and the cable used to send the maser signal to the FLFC laboratory were tested by sending the maser signal to the FLFC laboratory and then back to the fountain laboratory and comparing the frequency with the frequency directly in the fountain laboratory. The fractional stability of the maser distribution electronics measured in this way was  $4 \times 10^{-15}$  in ten seconds and showed a pronounced bump near 700 seconds (Fig. 5). This time scale of the increase in the noise is commensurate with the cycle of the air conditioning in the building.

### E. Statistical Uncertainties

The statistical uncertainties for the different frequency comparisons are shown in Fig. 6. The estimated statistical uncertainty of the  $\text{Hg}^+$  standard is far below that of the Cs standard (Fig. 5) and we would expect the uncertainties of

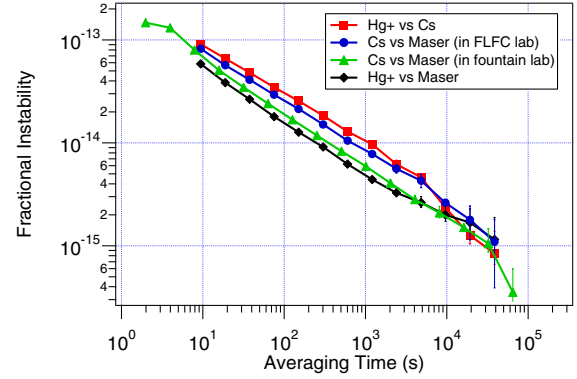


Fig. 6. Allan deviations for the frequency comparisons.

TABLE I

UNCERTAINTIES IN  $\text{Hg}^+$  FREQUENCY COMPARISON WITH CS NIST-F1 FREQUENCY STANDARD.

Source	Uncertainty [ $10^{-15}$ ]
Cs Standard	0.41
$\text{Hg}^+$ Standard	0.07
Gravitational Shift	0.1
<b>FLFC Uncertainties</b>	
Optical Uncertainties	< 0.01
Photodetection Uncertainties	0.03
Synthesizer Uncertainties	0.3
Analysis Uncertainties	0.04
Statistical Uncertainty	0.9
Final Uncertainty	1

the Cs standard to dominate. However, the uncertainty in the  $\text{Hg}^+/\text{Cs}$  comparison is larger than that of the Cs standard alone. The measurement of the maser frequency relative to the Cs standard performed in the FLFC lab was  $\approx 20\%$  higher than the measurement of the maser frequency relative to the Cs standard done in the fountain lab. A possible cause for this additional noise is the dead time in the counter [25]. Indeed, data taken at different gate times in the FLFC lab had uncertainties equal to the uncertainty measured in the fountain lab. Unfortunately, the majority of the data was taken with a gate time that exhibited additional noise.

The statistical error was determined by taking the standard deviation and dividing by the square root of the number of points. The fit of the fractional instability for the  $\text{Hg}^+$  frequency relative to Cs to  $A \tau^p$  yields a fractional instability of  $3.0 \times 10^{-13} \tau^{-0.50}$ , where  $\tau$  is the averaging time in seconds. Evaluating this for the total averaging time of the experiment gives a statistical uncertainty identical to that determined from the standard error.

### F. Final Uncertainties

A summary of the uncertainties is shown in Tab. I. The final result is limited by statistical uncertainties at the  $1 \times 10^{-15}$  level.

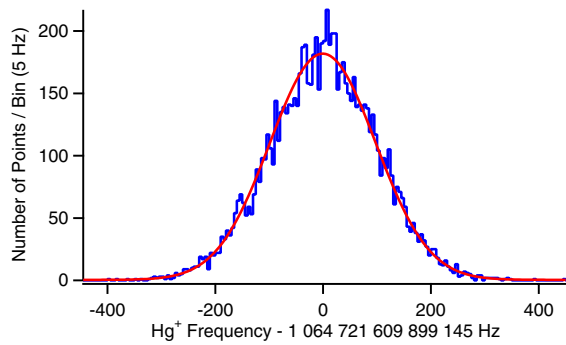


Fig. 7. Histogram of the  $\text{Hg}^+$  frequency with respect to the Cs standard with a Gaussian fit.

### G. H-Maser Comparison

The hydrogen maser used in the experiment is part of a collection of five masers that are periodically calibrated with respect to the Cs NIST-F1 standard [26]. The five masers are compared continuously to each other in order to determine the drifts of the masers and to calibrate their frequencies. The  $\text{Hg}^+$  frequency can therefore be determined directly from the frequency of the maser by use of the daily-averaged maser-maser calibration. This provides a redundancy check of the  $\text{Hg}^+$  frequency. The frequency obtained by this method agrees with that obtained with the Cs standard to  $5 \times 10^{-16}$ .

### H. Final Result

The final value for the most recent measurement of the  $\text{Hg}^+$  frequency standard is

$$f(\text{Hg}^+) = 1.064\,721\,609\,899\,145.89(1.06) \text{ Hz.} \quad (3)$$

This result is in agreement with the previously published values at the one sigma level [4]. A histogram of the 9.472-s data is shown in Fig. 7.

## V. PERSPECTIVE AND OUTLOOK

The uncertainty in the optical-to-microwave conversion process used in the measurement of the  $\text{Hg}^+$  optical frequency standard with respect to the Cs frequency standard remains below the statistical uncertainties of the measurement and the systematic uncertainties from the Cs standard. The dominant uncertainties in the optical-to-microwave conversion process are related to the photodetection of the repetition rate and the quality of synthesizer against which the repetition rate is compared. These uncertainties are not present in the comparison of two optical standards. Indeed, the uncertainty due to the optical synthesis process in the comparison of two optical standards will not rely on detecting the repetition rate, and the uncertainties related to the photodetection process and synthesizer will be eliminated. For such a comparison we estimate the uncertainty to be less than  $10^{-19}$ , well below the anticipated accuracies of the next generation of optical frequency standards.

## ACKNOWLEDGMENT

The authors thank T. Rosenband, D. Hume, D. Wineland, and J. Torgerson for their contributions to this work. This work is a contribution of NIST and is not subject to U.S. Copyright. Funding for this work was provided by NIST, NASA, and LANL.

## REFERENCES

- [1] Th. Udem, R. Holzwarth, T.W. Hänsch, "Optical frequency metrology," *Nature* vol. 416, pp. 233-237, 2002.
- [2] L. Hollberg, S. Diddams, A. Bartels, T. Fortier, and K. Kim, "The measurement of optical frequencies," *Metrologia*, vol. 42, pp. S105-S124, 2005.
- [3] T.M. Fortier, *et al.*, in preparation.
- [4] W.H. Oskay, S.A. Diddams, E.A. Donley, T. Fortier, T.P. Heavner, L. Hollberg, W.M. Itano, S.R. Jefferts, M.J. Jensen, K. Kim, F. Levi, T.E. Parker and J.C. Bergquist "A single-atom optical clock with high accuracy," to appear in *Phys. Rev. Lett.*, 2006.
- [5] Chr. Tamm, *et al.*, In these proceedings, 2006.
- [6] H.S. Margolis, G.P. Barwood, G. Huang, H.A. Klein, S.N. Lea, K. Szymaniec, and P. Gill, "Hertz-Level Measurement of the Optical Clock Frequency in a Single  $^{88}\text{Sr}^+$  Ion," *Science*, vol. 306, pp. 1355-1358, 2004.
- [7] E. Peik, B. Lipphardt, H. Schnatz, T. Scheider, Chr. Tamm, S.G. Karshenboim, "Limit on the present temporal variation of the fine structure constant," *Phys. Rev. Lett.*, vol. 93, pp. 170801/1-4, 2004.
- [8] M. Fischer, N. Kolachevsky, M. Zimmermann, R. Holzwarth, Th. Udem, T.W. Hänsch, M. Abgrall, J. Grünert, I. Maksimovic, S. Bize, H. Marion, F. Pereira Dos Santos, P. Lemonde, G. Santarelli, M. Hass, U.D. Jentschura, and C.H. Keitel, "New Limits on the Drift of Fundamental Constants from Laboratory Measurements," *Phys. Rev. Lett.* vol. 92, pp. 230802/1-4, 2004.
- [9] T.P. Heavner, S.R. Jefferts, E.A. Donley, J.H. Shirley, and T.E. Parker, "Recent Improvements in NIST-F1 and a Resulting Accuracy of  $\delta f/f = 0.61 \times 10^{-15}$ ," *IEEE Trans. Inst. and Meas.*, vol. 54, pp. 842-845, 2005.
- [10] T.P. Heavner, S.R. Jefferts, E.A. Donley, J.H. Shirley, and T.E. Parker, "NIST F1: recent improvements and accuracy evaluations," *Metrologia*, vol. 42, pp. 411-422, 2005.
- [11] S.R. Jefferts, J. Shirley, T.E. Parker, T.P. Heavner, D.M. Meekhof, C. Nelson, F. Levi, G. Costanzo, A. De Marchi, R. Drullinger, L. Hollberg, W.D. Lee, and F.L. Walls, "Accuracy evaluation of NIST-F1," *Metrologia* vol. 39, pp. 321-336, 2002.
- [12] S.A. Diddams, Th. Udem, J.C. Bergquist, E.A. Curtis, R.E. Drullinger, L. Hollberg, W.M. Itano, W.D. Lee, C.W. Oates, K.R. Vogel, and D.J. Wineland, "An Optical Clock Based on a Single Trapped  $\text{Hg}^+$  Ion," *Science* vol. 293, pp. 825-828, 2001.
- [13] B.C. Young, R.J. Rafac, J.A. Beall, F.C. Cruz, W.M. Itano, D.J. Wineland, and J.C. Bergquist, " $\text{Hg}^+$  Optical Frequency Standard: Recent Progress," in proceedings *XIV International Conference on Laser Spectroscopy*, edited by R. Blatt (World Scientific, Austria, 1999).
- [14] J. Reichert, R. Holzwarth, Th. Udem, and T.W. Hänsch, "Measuring the frequency of light with mode-locked lasers," *Opt. Commun.* vol. 172, pp. 59-68, 1999.
- [15] T.M. Fortier, A. Bartels and S.A. Diddams, "Octave-spanning Ti:sapphire laser with a repetition rate  $> 1$  GHz for optical frequency measurements and comparisons," *Opt. Lett.* vol. 31, pp. 1011-1013, 2006.
- [16] D.J. Jones, S.A. Diddams, J.K. Ranka, A. Stentz, R.S. Windeler, J.L. Hall, and S.T. Cundiff, "Carrier-Envelope Phase Control of Femtosecond Mode-Locked Lasers and Direct Optical Frequency Synthesis," *Science*, vol. 288, pp. 635-639, 2000.
- [17] J.K. Ranka, R.S. Windeler, A.J. Stentz, "Visible continuum generation in air silica microstructure optical fibers with anomalous dispersion at 800 nm," *Opt. Lett.*, vol. 25, pp. 25-27, 2000.
- [18] P.O. Schmidt, T. Rosenband, C. Langer, W.M. Itano, J.C. Bergquist, and D.J. Wineland, "Spectroscopy using quantum logic," *Science* vol. 309, pp. 749-752, 2005.
- [19] B.C. Young, F.C. Cruz, W.M. Itano, J.C. Bergquist, "Visible Lasers with Subhertz linewidths," *Phys. Rev. Lett.* vol. 82, 3799-3802 (1999).
- [20] L-S. Ma, Z. Bi, A. Bartels, L. Robertsson, M. Zucco, R.S. Windeler, G. Wilpers, "Optical Frequency Synthesis and Comparison with Uncertainty at  $10^{-19}$  Level," *Science*, vol. 303, pp. 1843-1845, 2004.

- [21] M. Zimmermann, C. Gohle, R. Holzwarth, Th. Udem, and T.W. Hänsch, "Optical clockwork with an offset-free difference-frequency comb: accuracy of sum- and difference-frequency generation," *Opt. Lett.*, vol. 29, pp. 310, 2004.
- [22] E.N. Ivanov, S.A. Diddams, and L. Hollberg, "Analysis of Noise Mechanisms Limiting the Frequency Stability of Microwave Signals Generated with a Femtosecond Laser," *IEEE J. Sel. Top. in Quant. Electron.*, vol. 9, pp. 1059-1065, 2003.
- [23] L-S. Ma, Z. Bi, A. Bartels, K. Kim, L. Robertsson, M. Zucco, R.S. Windeler, G. Wilpers, C. Oates, L. Hollberg, and S.A. Diddams, "Frequency uncertainty for optically-referenced femtosecond laser frequency combs," to be published in *IEEE J. Quant. Elect.*, 2006.
- [24] T.P. Heavner, S.R. Jefferts, E.A. Donley, T.E. Parker, and F. Levi, "A New Microwave Synthesis Chain for the Primary Frequency Standard NIST-F1," *2005 IEEE International Frequency Control Symposium and Exhibition*, 2005.
- [25] P. Lesage, "Characterization of Frequency Stability: Bias Due to the Juxtaposition of Time-Interval Measurements," *IEEE Trans. Inst. and Meas.*, vol. IM-32, pp. 204-207, 2003.
- [26] T.E. Parker, S.R. Jefferts, T.P. Heavner, and E.A. Donley "Operation of the NIST-F1 caesium fountain primary frequency standard with a maser ensemble, including the impact of frequency transfer noise," *Metrologia*, vol. 42, pp. 423-430, 2005.